

**CRYSTAL STRUCTURE AND CHEMICAL COMPOSITION OF A PRESOLAR SILICATE FROM THE QUEEN ELIZABETH RANGE 99177 METORITE.** A. N. Nguyen<sup>1,2</sup>, L. P. Keller<sup>1</sup>, Z. Rahman<sup>1,2</sup>, and S. Messenger<sup>1</sup>. <sup>1</sup>Robert M. Walker Laboratory for Space Science, ARES, NASA JSC, Houston TX, <sup>2</sup>ESCG/Jacobs Technology, Houston, TX ([lan-anh.n.nguyen@nasa.gov](mailto:lan-anh.n.nguyen@nasa.gov)).

**Introduction:** Mineral characterization of presolar silicate grains, the most abundant stardust phase, has provided valuable information about the formation conditions in circumstellar environments and in supernova (SN) outflows. Spectroscopic observations of dust around evolved stars suggest a majority of amorphous, Mg-rich olivine grains, but crystalline silicates, most of which are pyroxene, have also been observed [1]. The chemical compositions of hundreds of presolar silicates have been determined by Auger spectroscopy and reveal high Fe contents and nonstoichiometric compositions intermediate to olivine and pyroxene [2-6]. The unexpectedly high Fe contents can partly be attributed to secondary alteration on the meteorite parent bodies, as some grains have Fe isotopic anomalies from their parent stellar source [7].

Only about 35 presolar silicates have been studied for their mineral structures and chemical compositions by transmission electron microscopy (TEM). These grains display a wide range of compositions and structures, including crystalline forsterite, crystalline pyroxene, nanocrystalline grains, and a majority of amorphous nonstoichiometric grains. Most of these grains were identified in the primitive Acfer 094 meteorite. Presolar silicates from this meteorite show a wide range of Fe-contents, suggestive of secondary processing on the meteorite parent body. The CR chondrite QUE 99177 has not suffered as much alteration [8] and displays the highest presolar silicate abundance to date among carbonaceous chondrites [3, 6]. However, no mineralogical studies of presolar silicates from this meteorite have been performed. Here we examine the mineralogy of a presolar silicate from QUE 99177.

**Experimental:** A separate of QUE 99177 fine-grained matrix material was prepared by gentle freeze-thaw disaggregation and ultrasonication. Soluble organic material was removed and grains were separated by centrifugation. These grains were dispersed on clean Au foil from liquid suspension and analyzed by O and Si isotopic imaging in the JSC NanoSIMS 50L to identify anomalous O-rich grains. Measurements of  $20 \times 20 \mu\text{m}^2$  regions were conducted using a  $\sim 0.8$  pA,  $\sim 100$  nm  $\text{Cs}^+$  primary ion beam, and  $^{24}\text{Mg}^{16}\text{O}$  was collected along with the O and Si isotopes as negative secondary ions.

An  $^{17}\text{O}$ -rich grain was selected for TEM analysis. This grain (3\_59\_4) is  $\sim 360 \times 280$  nm in plane view (Fig. 1). An electron transparent cross-section was pro-

duced by focused ion beam (FIB) milling. The sample was coated with 10 nm of Au to minimize charging. A C cap was deposited on the grain of interest to serve as a marker and to protect the grain. Electron beam deposited Pt was then placed over the grain before a  $8 \mu\text{m}$  long Pt strap was placed over the section to be lifted out. A portion of the section containing the presolar grain is shown in Fig. 1. Imaging, structural and chemical data were obtained with the JSC JEOL 2500 field-emission scanning transmission electron microscope. Elemental maps were obtained with a Noran thin window energy-dispersive X-ray (EDX) spectrometer using a 2 nm incident probe. Grain crystallinity was investigated by electron diffraction and dark-field imaging.

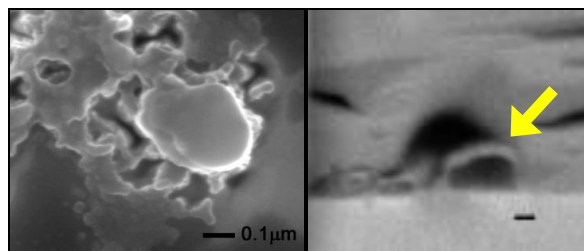


Figure 1. FE-SEM image of presolar silicate 3\_59\_4 (left). Backscatter electron image of grain cross-section (right). Scale bars are 100 nm.

**Results:** The presolar silicate is enriched in  $^{17}\text{O}$  ( $\delta^{17}\text{O} = 570$  ‰) and depleted in  $^{18}\text{O}$  ( $\delta^{18}\text{O} = -240$  ‰). This isotopic signature is indicative of condensation in low-mass red giant branch (RGB) or asymptotic giant branch (AGB) stars. The grain has isotopically normal Si composition. From the NanoSIMS analysis, the grain appears more Si- and Mg-rich than the surrounding matrix grains. In cross-section, the grain is ovoid and extends  $\sim 165$  nm below the surface (Fig. 2). Selected area electron diffraction (SAED) shows the grain contains a nanocrystalline core (triangular region in Fig. 2) and an amorphous shell. The core is stoichiometric enstatite ( $\text{MgSiO}_3$ ) and the electron diffraction pattern is consistent with nanocrystalline enstatite. The underbelly of the grain is slightly depleted in Mg [ $\text{Mg}/\text{Si}$  (at.)  $\sim 0.7$ ] and contains minor Fe [ $\text{Mg}/(\text{Mg}+\text{Fe})$  (at.)  $= 0.95$ ].

**Discussion:** Microstructural studies of AGB silicate stardust grains are consistent with spectroscopic observations, finding that most of the grains are amorphous. However, some FIB-extracted grains are so small that ion beam amorphization cannot be excluded. Most of the silicate stardust grains are nonstoichio-

metric and more Fe-rich than expected. Again, some of this Fe was likely acquired during parent body alteration. There are no clear systematic differences in the microstructures of SN and AGB silicates, as the grains are all quite diverse from one another. About a third of the silicates analyzed by TEM are crystalline, but most of these grains are Mg-rich olivine [9-13], in contrast to spectroscopic observations of crystalline pyroxene. Prior to this study, only 3 presolar pyroxene grains had been identified. One is an amorphous, stoichiometric (En100) SN condensate that likely condensed as a crystal and was later amorphized [14]. One AGB pyroxene with an unusual high-pressure crystal structure may have experienced shock processing [15]. A twinned clinoenstatite grain (En99) with an  $^{17}\text{O}$  enrichment comparable to silicate 3\_59\_4 was identified as part of an assemblage that included an Al-rich silicate and a probable oxide grain [14]. This silicate likely formed at high temperature and was rapidly quenched.

The chemical composition and nanocrystalline core of silicate 3\_59\_4 suggest it also could have condensed as a single crystal, but was later amorphized in the interstellar medium (ISM) by irradiation. The Fe in the outer portions of the grain could have been acquired from alteration on the parent body. Possible evidence of processing in the ISM has also been observed in a presolar olivine having a crystalline core and amorphous Fe-rich rim [10]. These authors favor amorphization and Mg removal by sputtering in the ISM. Given the observance of Fe infiltration from meteorite matrix material however [7], the Fe could have been acquired through parent body processing.

Low-energy irradiation experiments of crystalline olivine have resulted in amorphization of the grain and chemical alteration to pyroxene-like compositions [16]. However, this does not appear to be a viable explanation for the present grain, whose crystalline core is pyroxene rather than olivine. Thermodynamic models of olivine condensation predict a crystalline core and thick amorphous mantle if a large portion of the grain condensed at lower temperatures [17]. A higher Fe content in the grains' exterior is also predicted if the gas becomes greatly depleted in Mg. However, this scenario is unlikely given that the amorphous portion of the grain is nearly stoichiometric.

**References:** [1] Molster F. and Kemper C. (2005) *Space Sci. Rev.*, 119, 3-28. [2] Nguyen A.N. et al. (2007) *Astrophys. J.*, 656, 1223-1240. [3] Floss C. and Stadermann F. (2009) *Geochim. Cosmochim. Acta*, 73, 2415-2440. [4] Vollmer C. et al. (2009) *Geochim. Cosmochim. Acta*, 73, 7127-7149. [5] Bose M. et al. (2010) *Astrophys. J.*, 714, 1624-1636. [6] Nguyen A.N. et al. (2010) *Astrophys. J.*, 719, 166-189. [7] Floss C. and Stadermann F.J. (2012) *Meteorit. Planet.*

*Sci.*, 47, 992-1009. [8] Abreu N.M. and Brearley A.J. (2010) *Geochim. Cosmochim. Acta*, 74, 1146-1171. [9] Keller L.P. and Messenger S. (2011) *Geochim. Cosmochim. Acta*, 75, 5336-5365. [10] Vollmer C. et al. (2009) *Astrophys. J.*, 700, 774-782. [11] Busemann H. et al. (2009) *Earth & Planet. Sci. Lett.*, 288, 44-57. [12] Messenger S. et al. (2003) *Science*, 300, 105-108. [13] Messenger S. et al. (2005) *Science*, 309, 737-741. [14] Nguyen A.N. et al. (2010) *Meteorit. Planet. Sci.*, 45, A5423. [15] Vollmer C. et al. (2007) *Astrophys. J.*, 666, L49-L52. [16] Demyk K. et al. (2001) *Astron. Astrophys.*, 368, L38-L41. [17] Gail H.-P. and Sedlmayr E. (1999) *Astron. Astrophys.*, 347, 594-616.

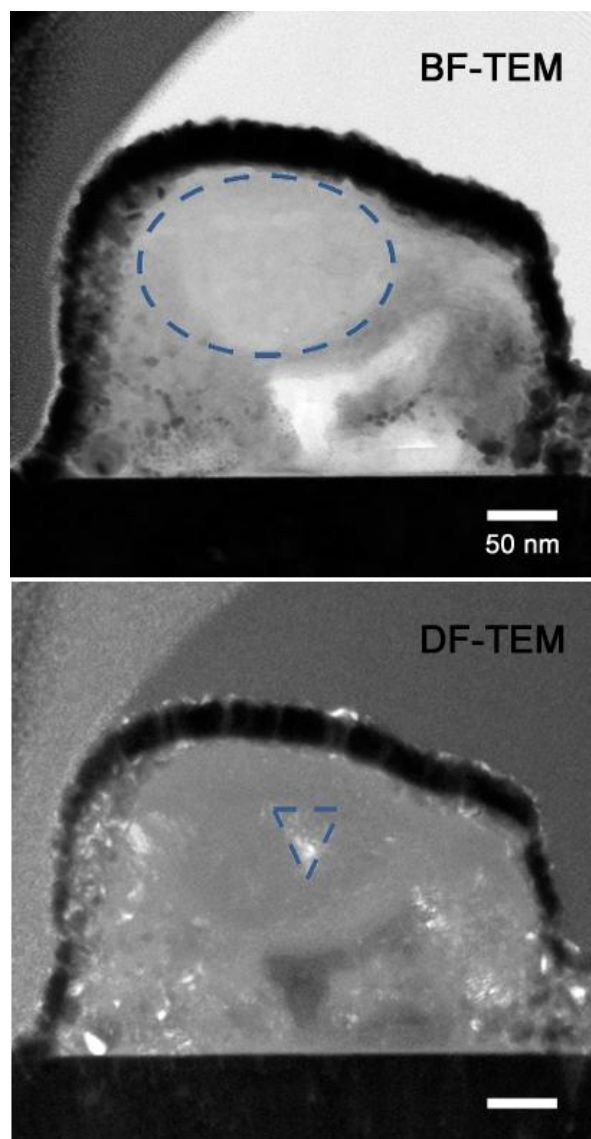


Figure 2. Bright- and dark-field TEM images of silicate 3\_59\_4. The central deltoid seen in the DF image is nanocrystalline enstatite. The surrounding amorphous material contains minor Fe.